IOP Conf. Series: Materials Science and Engineering **724** (2020) 012063 doi:10.1088/1757-899X/724/1/012063

# Technological and structural analysis of $Al_2O_3$ $40TiO_2$ coating deposited on a shaft sleeve of hydraulic pump

**C Cîrlan Paleu[1], B Istrate[1], V Paleu[1] and C Munteanu[1]**
[1] Gheorghe Asachi Technical University of Iaşi, Mechanical Engineering Faculty, Mechanical Engineering, Mechatronics and Robotics Department, 63 D. Mangeron Blvd., 700050, Iaşi, RO, E-mail: cornelmun@gmail.com

**Abstract.** In the last decades, mechanical engineering applications have extensive use in many subdomains. Many researchers have used $Al_2O_3$ $40TiO_2$ (AMDRY6250) type coatings that have a wide use of plasma jets, significantly improving their wear, corrosion resistance and heat shock properties. It is especially used for hydraulic components such as pumps, impellers, and blowers. The performance of $Al_2O_3$ $40TiO_2$ layer is conditioned by a number of technological parameters of deposition, powder granulation and deposition incidence angle. In the present study, the authors will make sequential depositions of $Al_2O_3$ $40TiO_2$ on the surface of a material coming from a hydraulic system. Microstructural analysis of optical microscopy, scanning electron microscopy (SEM), and energy dispersive spectroscopy (EDAX) are performed both in the surface of the deposited material and in the section of the coated specimens, identifying the microstructure and the component phases. The authors highlighted the emergence of the "splat" type of formations that are specific to the ceramic coatings in the deposited layers and a good adhesion to the base material authorizing the use of this powder in the reconditioning of the hydraulic systems.

## 1. Introduction

Pumping station are vital key points of modern urban life, their continuously running in good state being a necessity for the people. Paleu et al. [1] analysed the main failures modes of pumping stations components. A weak spot of pumping stations are the pump themselves, especially their impellers, seals, bearings, casings, shafts, bushes, and sleeves. The latest of them (bushes and sleeves) can be easily reconditioned by proper choose of wear resistant coating materials and deposition method. In case of impellers and casings maintenance a special attention must be payed if coatings are used, as the thickness of these coatings can change the small interstitial space at the entrance of impellers, accentuating the cavitation phenomena [2-3].

Between coatings, $Al_2O_3$ $40TiO_2$ powder, also known as AMDRY6250, is recommended by producers for atmospheric plasma spray (APS) deposition on components of pumps. Recent research [4-11] indicated that there are few aspects known regarding the influence of aluminium titanate (Al2TiO5) in $Al_2O_3$-$TiO_2$ thermal spray coatings. Three $Al_2O_3$-$13TiO_2$ and three $Al_2O_3$- $40TiO_2$ from feedstock powder were analysed. The conclusion is the aluminium titanate ($Al_2TiO_5$/$Al_6Ti_2O_{13}$ ) can improve the hardness of $Al_2O_3$-$13TiO_2$ coating if found in the composition of feedstock powder, but it is detrimental to mechanical properties of $Al_2O_3$- $40TiO_2$. It was also underlined that it is possible to obtain Al2TiO5 during spraying, as long as it is provided a sufficient intermixing of the single oxides.

The behaviour of $Al_2O_3$–$40TiO_2$ and $Cr_3C_2$–20NiCr coatings deposited by HVOF spray technique on low cost carbon steel petroleum oil piping was studied by Zavareh et al. [5]. Results of corrosion and tribological tests show that $Al_2O_3$–40$TiO_2$ is superior to $Cr_3C_2$–20NiCr from corrosion resistance viewpoint, both coatings proving good resistance to wear. Vasudev et al. [6] deposited WC-Co-Cr and $Al_2O_3$ + 40$TiO_2$ coatings by detonation gun spray process on cast iron. Tribological tests revealed better wear behaviour of WC-Co-Cr. In XRD analysis of $Al_2O_3$ + 40$TiO_2$ coating can be observed the presence of aluminium titanate [6]. If results of [4] and [6] are correlated, the worse wear behaviour of $Al_2O_3$ + 40$TiO_2$ reported in [6] is explainable.

Znamirowski et al. [7] studied the field electron emission of $Al_2O_3$+13$TiO_2$ and $Al_2O_3$+40$TiO_2$. The study was intended for parabolic antenna application. Better emissivity of $Al_2O_3$+13$TiO_2$ is explained by thinner structure of the coating, composed by small spheres.

Positive results were related on hot corrosion resistance in aggressive environment of $Al_2O_3$+40$TiO_2$ coating on Superni 718 and AE 435 superalloys deposited by detonation gun method [8-9]. The application was envisioned for boilers and gas turbines components.

The microstructural transformations of TiO2, $Al_2O_3$+13$TiO_2$ and $Al_2O_3$+40$TiO_2$ at plasma spraying and laser engraving were presented in [10], $Al_2O_3$+40$TiO_2$ being the best candidate with low porosity (1.9%) and acceptable hardness ($HV_{0.3}$=1083).

Szala and Hejwowski [11] studied cavitation erosion resistance of flame-sprayed $Al_2O_3$-40%$TiO_2$/NiMoAl cermet coatings (low-velocity oxy-fuel (LVOF)), with respect to cavitation erosion mechanism versus feedstock powder ratio ($Al_2O_3$-$TiO_2$/NiMoAl). It seems that the structure of the obtained coating is very important on cavitation resistance, but a content increase up to 80% of $Al_2O_3$-$TiO_2$ in the feedstock powder was positive.

Modern pumps have their shafts and bushes made of AISI 303 (EN 1.4305) and AISI 316 (EN 1.4401), and their impellers, casings and sleeves of AISI 304 (EN 1.4301) and AISI 316 L (EN 1.4404). An economical method to obtain acceptable shaft sleeves is electrochemically deposition of chrome coatings, an element resistant to abrasive wear and corrosion. This paper studies the microstructure of the $Al_2O_3$+40$TiO_2$ coating deposited by APS technique in different number of layers (5, 7, and 9 layers) on steel samples from a reconditioned pump shaft sleeve. Microstructural investigations are welcome in selecting the best ceramic coating for pump components maintenance.

## 2. Experimental section

### *2.1. Materials*

The steel substrate belongs to a shaft sleeve of a vertical pump with electrochemically deposited chrome layer of thickness 100 μm. An examination of the pump shaft sleeve taken from years of exploitation proved that its surface had abrasive wear traces and even rusted parts (figure 1 and figure 2). These pumps are usually lubricated by processed water.

**Figure 1.** Worn shaft sleeve outer surface.

**Figure 2.** Cut worn shaft sleeve inner surface.

Parallelepipeds samples of 100 x 10 x 5 mm were cut from the shaft sleeve and chromed surface of the outer cylinder was completely removed by milling, its surface becoming flat. Samples preparation technology included sandblasting and polishing. Coated pads are made by atmospheric plasma spray (APS) deposition of $Al_2O_3$ $40TiO_2$ (AMDRY6250) on steel substrate.

Three coated flat samples were realised with different number of $Al_2O_3$ $40TiO_2$ deposited layers: 5, 7, and 9. These samples will be denoted as P1, P2, and P3, respectively.

### *2.2. Atmospheric Plasma Spray (APS) equipment and optimum deposition parameters*

Table 1 presents the technological parameters used for the APS coating process.

**Table 1.** Technological parameters used for coating process.

| Powder | Gun | Ar | | $H_2$ | | Electric | | Powder feeder 9MP | | | Spray distance (inch) |
|---|---|---|---|---|---|---|---|---|---|---|---|
| | | Pressure (psig) | Gas flow (SCFH) | Pressure (psig) | Gas flow (SCFH) | DC (A) | DC (V) | Carrier gas flow (SCFH) | Air Preasure (psig) | Rate (lb/h) | |
| Al2O3 40TiO2 coating | 9MB | 75 | 110 | 50 | 10 | 500 | 60-70 | 13.5 | 20 | 5.6 | 4.5 |

### *2.3. Methods of analysis*

The deposited coating surfaces for the three different samples (P1, P2 and P3) were analyzed by optical microscopy, scanning electron microscopy (SEM), and Energy Dispersive Spectroscopy (EDAX). SEM microscopy was used also for transversal images acquisition of different AMDRY6250 coatings.

## 3. Results

### *3.1. Results of optical microscopy*

Figure 3 highlights the optical microstructure of the base material at different magnification powers. A recrystallized biphasic structure consisting of ferrite alpha and perlite grains is highlighted. The grain distribution is relatively uniform, with slight parallel orientations of alpha ferrite grains.

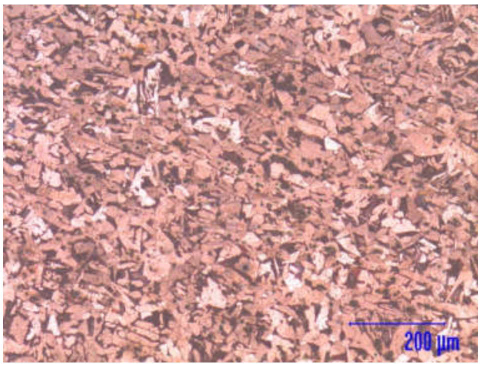


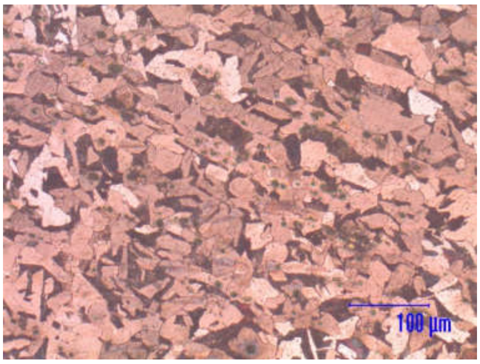


**a)** **b)**

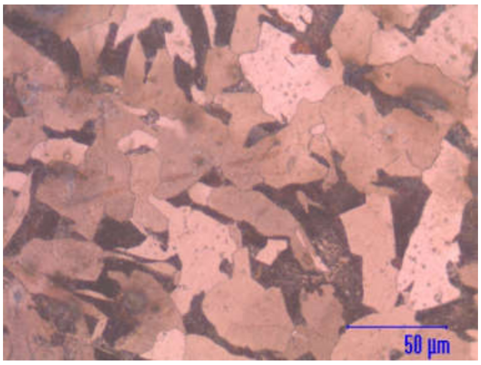


**c)**

**Figure 3.** Optical images of based material microstructure: a) 100X; b) 200X; c) 500X.

### *3.2. SEM analysis of coated surfaces*

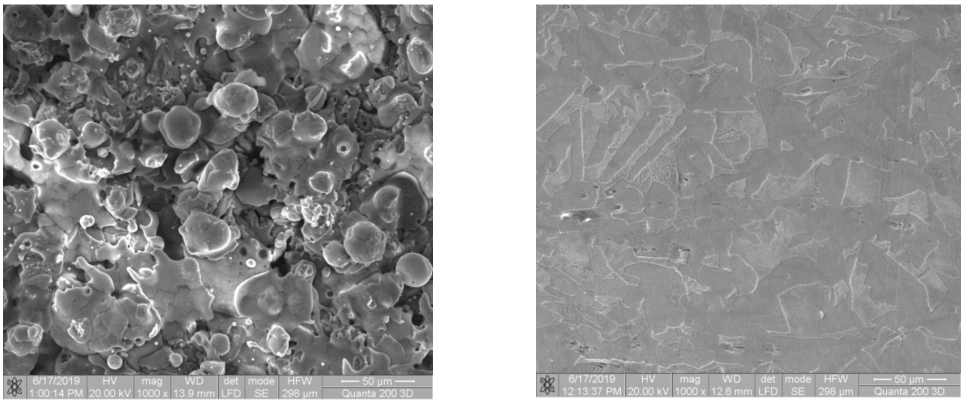

**a)** **b)**

**Figure 4.** SEM images of surface of the experimental samples: a) coated surface; b) uncoated surface.

In figure 4, SEM images indicate the morphology of the coated surface compared to the base material. These are similar with the optical micrographs and the surface of the deposited coating indicates the presence of a partially homogeneous layer with highlighting of some microcracks and unmelted particles.

The presence of microcracks may also be due to the different thermal contraction coefficient between the base material and the Al2O3-TiO2-coated layers during the cooling process.

### *3.3. Cross-section SEM analysis of coatings*

The cross-section scanning electron images in figures 5, 6 and 7 reveal the morphology appearance of the coated samples. The thickness variation is between 55 microns (5 passes) and 116 microns (9 passes) - Table 2. It results that a single pass of the spraying process produces a layer thickness of about 12 microns. In all three cases the layers are adhered to the base material. The structure is specific to ceramic coatings with the presence of oxides in the form "splats" type due to successive passes during the deposition process.

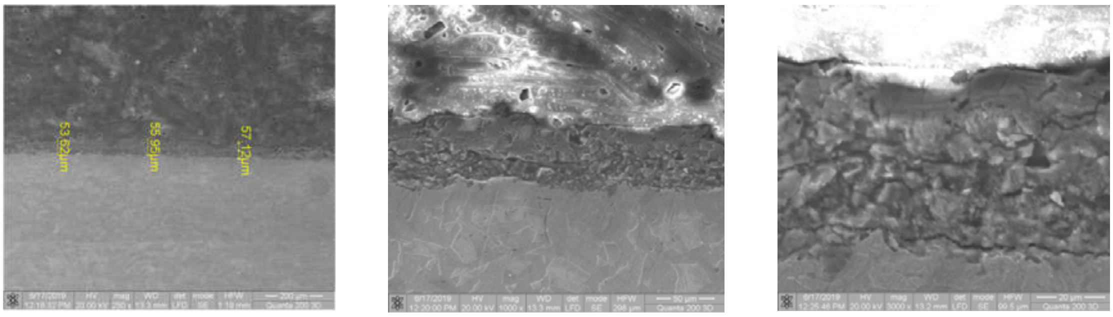


a) b) c)

**Figure 5.** Cross-section SEM images of 5 passes coated sample: a) 250X; b) 1000X; c) 3000X.

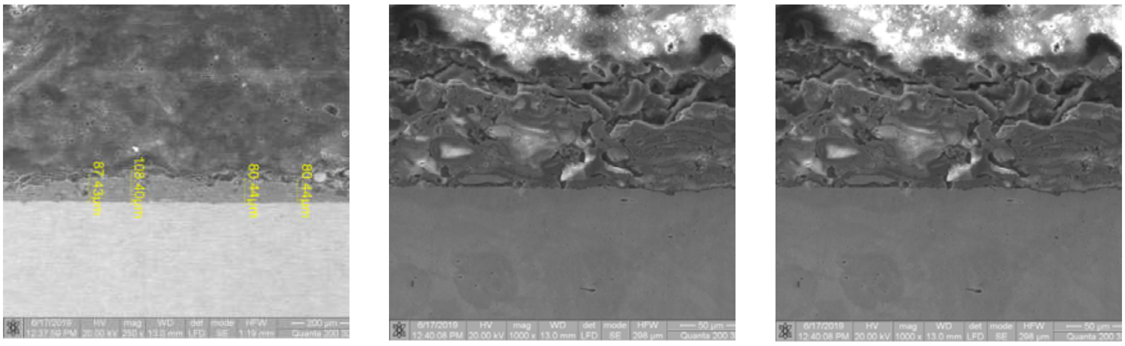


a) b) c)

**Figure 6.** Cross-section SEM images of 7 passes coated sample: a) 250X; b) 1000X; c) 3000X.

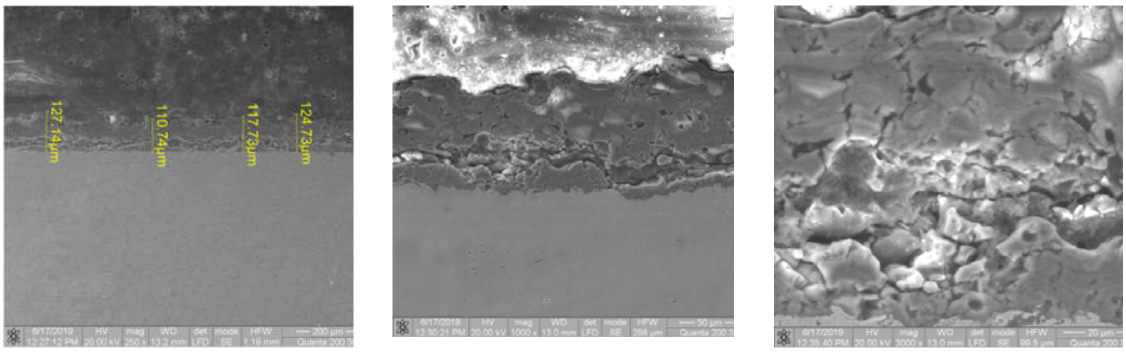


a) b) c)

**Figure 7.** Cross-section SEM images of 9 passes coated sample: a) 250X; b) 1000X; c) 3000X.

**Table 2.** Measurements of coating thicknesses.

| Coatings | 5 passes | 7 passes | 9 passes |
|---|---|---|---|
| Average thickness (µm) | 55.56 | 87.89 | 116.58 |

*3.4. EDAX analysis*

Table 3 presents the chemical compositions and the distribution of the elements in the coatings section. Al, O, and Fe are evenly distributed in the base matrix, whereas titanium is found in isolated areas of the ceramic layer.

**Table 3.** Chemical compositions of the coated samples.

| Chemical Elements (%wt.) | %O | %Al | %Ti | %Fe |
|---|---|---|---|---|
| 5 passes | 27.11 | 44.92 | 05.60 | 22.38 |
| 7 passes | 29.80 | 46.06 | 07.73 | 16.41 |
| 9 passes | 30.09 | 45.13 | 08.63 | 16.14 |

## 4. Conclusions

Different thickness layers of $Al_2O_3$ $40TiO_2$ (AMDRY 6250) were deposited by APS method on flat steel samples obtained from reconditioned shaft sleeve of a vertical pump. The quality of 5, 7 and 9 passes of coatings was analysed by optical microscopy, scanning electron microscopy (SEM), and Energy Dispersive Spectroscopy (EDAX).

The results show that the coatings are relatively homogenous and adherent to substrate. The thickness varies between 55 microns and 116 microns. The coatings produces by atmospheric plasma spraying (APS) are composed by individual splats of fast solidified spray powder particles. The presence of microcracks may also be due to the different thermal contraction coefficient between the base material and the $Al_2O_340TiO_2$-coated layers during the cooling process.

## 5. References

[1] Paleu Cîrlan C, Paleu V, Istrate B, Cimpoesu N and Munteanu C 2019 *IOP Conf. Series: Mater. Sci. Eng.* **591:012007** DOI: 10.1088/1757-899X/591/1/012007
[2] Bloch H P and Budris A R 2014 *Pump user's handbook life extension* - 4$^{th}$ Ed. (Lilburn: The Fairmont Press / Taylor & Francis) p 556
[3] Budris A R 2013 *WaterWorld* **28 – 4** 18
[4] Richter A, Berger L-M, Conze S, Sohn Y J and Vaßen R 2019 I*OP Conf. Series: Mater. Sci. Eng.* **480:012007**
[5] Zavareh M A et al. 2016 *Ceramics Int.* **42** (4) 5203-5210
[6] Vasudev H, Thakur L, Singh H and Bansal A 2018 *Kovove Mater.* **56** 55–63
[7] Znamirowski Z, Pawlowski L, Cichya T and Czarczynski W. 2004 *Surf. & Coat. Technol.* **187** 37–46
[8] Mishra N K, Kumar Naveen and Mishra S B 2014 *Indian J. Mater. Sci.*, **Article ID 453607**, 5 p., http://dx.doi.org/10.1155/2014/453607
[9] Mishra N K and Mishra S B 2015 *Bull. Mater. Sci.* **38** 7 1679–1685
[10] Tomaszek R, Pawlowski L, Zdanowski J, Grimblot J and Laureyns 2004 *Surf. & Coat. Technol.* **185** 137–149
[11] Szala M and Hejwowski T 2018 *Coatings* **8** 254; doi:10.3390/coatings8070254